J Porous Mater (2015) 22:219–228
DOI 10.1007/s10934-014-9888-2

Effects of organic templates on the structural properties of porous clay heterostructures: a non-micellar template model for porous structure

Yuebo Wang · Xiaoqin Lin · Ke Wen · Jianxi Zhu · Hongping He

Published online: 22 November 2014

Abstract In this study, a series of surfactants with different chain lengths were used to investigate the effect of organic templates on the structural properties of porous clay heterostructures (PCH). The variation tendencies of structural properties and chemical component were characterized by X-ray diffraction, CHN elemental analysis, major element analysis, and nitrogen adsorption/desorption at −196 °C. Non-local density functional theory was employed to characterize pore size distributions in both micropore and mesopore regions owing to the bi-model pore structures of PCH. The major textural parameters of PCH samples increased with increasing the chain length and the intercalated amount of template agent, while the most probable pore size remained unchanged around 1.3–1.4 nm. Based on the structural and chemical component results of PCH, a non-micellar template model was presented to explain the formation mechanism of porous structure. By the extrusion and occupation of polymerizate of TEOS within interlayer, a fixed number of hydrocarbon chains congregate together to form surfactant aggregates (template). The aggregates with different chain lengths cause the increase of pore volume in depth dimension rather than in diameter. The obtained results also shed some light on the different roles of inorganic base clay and organic template agents in the formation of porous structure. Montmorillonite as the inorganic host supplies the space for pillaring reaction and controls the arrangement of template agent within interlayer. As the template agent and modifying agent, the cationic surfactant is the dominant factor in forming pores relative to amine. The neutral amine mainly serves as catalyst for the polymerization of TEOS besides its co-template effect.

Keywords Porous clay heterostructures · Non-local density functional theory · Combined micro- and mesoporosity · Surfactant alkyl chain length

Y. Wang · X. Lin · K. Wen · J. Zhu (✉) · H. He
CAS Key Laboratory of Mineralogy and Metallogeny, Guangzhou Institute of Geochemistry, Chinese Academy of Sciences, 511 Kehua Street, Wushan, Tianhe District, Guangzhou 510640, China
e-mail: zhujx@gig.ac.cn

Y. Wang
e-mail: wangyuebo@gig.ac.cn

X. Lin
e-mail: linxiaoqin@gig.ac.cn

K. Wen
e-mail: wenke@gig.ac.cn

H. He
e-mail: hehp@gig.ac.cn

Y. Wang · X. Lin · K. Wen
University of Chinese Academy of Sciences, Beijing 100049, China

Y. Wang · X. Lin · K. Wen · J. Zhu · H. He
Guangdong Provincial Key Laboratory of Mineral Physics and Materials, 511 Kehua Street, Guangzhou 510640, China

1 Introduction

Mesoporous materials have been attracting great attentions for their potential applications as catalysts and adsorbents. Many studies have been conducted to synthesize mesoporous materials, such as SBA-15 [1] and FDU-5 [2], since the invention of M41S family [3]. Generally, cationic surfactants are used as template agents in the synthesis of mesoporous materials. The cationic surfactants, meanwhile, are also often used in the organic intercalation of inorganic clay minerals. Inspired by the use of cationic

surfactants in the preparation of M41S family, porous clay heterostructures (PCH) was first synthesized by Galarneau et al. [4] in 1995 from fluorohectorite and surfactants with different chain lengths to generate mesoporous silica framework within interlayer space of clay. PCH belong to a kind of pillared clay according to the definition of IUPAC [5] because of their chemical and thermal stability, large specific surface area and unique combined micro- and mesoporosity.

Recent studies about PCH have been focused on their application for catalysis [6–8], adsorption [9–11], carrier [12] and template [13–15]. To yield the final products with desired surface properties in their specific applications, especially textural properties for porous materials, it is necessary to fully understand the correlation between the preparation condition and resultant structural properties. The template agent plays an important role in the porosity of porous materials. In the work of Galarneau et al. [4], pore size of the final product obtained by Horvath–Kawazoe (HK) analysis increased from 15 to 22 Å with increasing the chain length of neutral amine containing from 6 to 12 carbon atoms. When the hydrocarbon chain of quaternary ammonium cation (QAC^+) was prolonged from 10 to 16 carbon atom, pore size enlarged 1 Å. Based on their results, they proposed a model for formation of porous structure of PCH. In the proposal, micelle were formed from the intercalated cationic surfactant and neutral amine within interlayer of clay mineral host; the pore size was controlled by adjusting micellar size and volume. In other papers, some authors also found the longer chain length had the positive effect on major textural parameters of PCH including pore size evaluated by Broekhoff–De Boer method and Grenkel-Halsey-Hill equation [16], whereas some others found the chain length of template had little relevancy with textural properties [10]. Furthermore, only a few type of surfactant with different chain length was used in these previous works, which were not sufficient to explain the effect of template agent on porous structure. Moreover, the different contributions of cationic surfactant and neutral amine to textural properties and the roles of inorganic base clay and organic templates in the formation of porous structure were ignored in previous research.

It is well known, the pore size distributions (PSD) of PCH are in the range of the transition between micro and mesopores. Thus, it is possible to derive all the porosity information over this dimensional range in the solids at the same time from PSD plots [17, 18]. Generally, the PSD of PCH are evaluated by BJH method [19, 20] and HK analysis [4]. In principle, the classic macroscopic thermodynamic methods, including Barrett–Joyner–Halenda (BJH) method and Dubinin–Radushkevich (DR) equation, are only applicable to a specific pore size range. In contrast, the density functional theory (DFT) is independent of capillary condensation. This method can be applied across the complete micropore–mesopore range, which has a great advantage compared to other textural analysis methods. Zhu et al. [18] employed DFT method to characterize the PSD of PCH. Their results illustrated that the method was appropriate for evaluating such bi-model porous structure. However, DFT method was not employed to study the correlation between the chain length of template agent and the structural properties of PCH.

In this work, PCH samples are prepared with a series of surfactants with different chain lengths. Non-local density functional theory (NLDFT) was employed to characterize PSD in both micropore and mesopore regions. The aim of this study is to investigate the effect of template agents on the structural properties of PCH, with the goal to disclose the mechanism for the formation of porous structure of PCH and to determine the different roles of inorganic base clay and long-chain organic agents in the formation of porous structure.

2 Experiment

2.1 Materials

Montmorillonite (Mt) obtained from Inner Mongolia, China, showed the very high purity above 95 % containing quartz as an impurity by XRD measurement. Its chemical compositions (wt%) were as follows: SiO_2 58.16 %, Al_2O_3 16.95 %, Fe_2O_3 5.26 %, CaO 2.29 %, MgO 3.57 %, Na_2O 0.19 %, K_2O 0.15 %, MnO 0.0 %, TiO_2 0.20 %, P_2O_5 0.08 %, and the ignition loss 13.12 %. The cation exchange capacity (CEC) was 110.5 mmol/100 g measured through hexammine cobalt (III) cation exchanging method [21, 22]. Octyltrimethylammonium chloride (OTAC, approx. 99 %), decyltrimethylammonium bromide (DTAB, approx. 99 %), dodecyltrimethylammonium chloride (DDTAC, approx. 99 %), tetradecyltrimethylammonium chloride (TDTAC, approx. 99 %), cetyltrimethylammonium bromide (CTAB, approx. 99 %) and stearyltrimethylammoium bromide (STAB, approx. 99 %) were purchased from Nanjing Robiot Co., Ltd. Octylamine (approx. 99 %) and tetradecylamine (approx. 96 %) were purchased from Aladdin chemistry Co., Ltd. Dodecanamine (approx. 98 %) was purchased from Sigma-Aldrich chemistry Co., Ltd. Tetraethylorthosilicate (TEOS, chemically pure) was purchased from Guangzhou chemical reagent factory.

2.2 Synthesis of PCH samples

The first step is to prepare the organic clay. The interlayer calcium cations were exchanged for cationic surfactant [$C_mH_{2m+1}N(CH_3)_3Br/Cl$, m = 8, 10, 12, 14, 16, and 18] whose amount was l times (l = 0.5, 1.0, 2.0, and 4.0) the

CEC of Mt. The mixture was then stirred at 80 °C for 10 h. Followed by filtration, the obtained organo-montmorillonite (OMt) was washed with distilled water to remove excess water-soluble surfactant. Subsequently, the OMt was air dried at 80 °C and ground sufficiently to pass 100-mesh sieve. The resultant product is referred as Mt-lCm. In the following step, OMt was mixed with neutral amine ($C_nH_{2n+1}NH_2$, n = 8, 12, and 14) and TEOS with the mass ratio of OMt/neutral amine/TEOS of 1/1/120. After the continuous stirring for 4 h at 60 °C, the modified clay was separated by filtration with no washing, air dried overnight at 80 °C and finally calcined at 550 °C for 6 h. The final product is designated as P-lCmNn.

2.3 Characterization methods

X-ray diffraction (XRD) patterns were obtained using a Bruker D8 Advance diffractometer with a Ni filter and Cu Kα radiation (λ = 0.154 nm) generated at 40 kV and 40 mA. The scan rate was 2° (2θ) min^{-1}.

The CHN elemental analysis were performed using an Elementar Vario EL III Universal CHNOS Elemental Analyzer. The AMT content (in g per g clay mineral) was calculated as MAMT = WN/K, where K is the content of N in the AMT, and WN is the mass percentage of N in the AMT determined from the CHN analysis. Major element oxides were analyzed using a Rigaku RIX 2000 X-ray fluorescence spectrometer (XRF) on fused glass beads. Calibration lines used in quantification were produced by bivariate regression of data from 36 reference materials encompassing a wide range of silicate compositions, and analytical uncertainties are mostly between 1 and 5 %. The details of the analytical procedures can be found in Zhang et al. [23].

Nitrogen adsorption/desorption isotherms were measured at −196 °C using a Micromeritics ASAP 2020 instrument. Prior to analysis, samples were outgassed at 120 °C for 12 h. The specific surface area was calculated by the BET equation and the total pore volume was evaluated from nitrogen uptake at a relative pressure of 0.97 [24]. The DA equation method was used to calculate the microporous specific surface area and micropore volume [25]. The NLDFT method for pillared clay was used to carry out the PSD analysis [26].

3 Results and discussion

3.1 Structural characteristics and chemical component of PCH samples

3.1.1 XRD analysis

X-ray diffraction is demonstrated as a credible technique for the determination of the basal spacing of intercalated clay [27, 28]. In this work, three reflections are observed in the XRD patterns of PCH samples (Fig. 1). Smectites are characterized by non-basal reflections, such as (02, 11), (13, 20), (04, 22), (15, 24, 31) and (06, 33) bands, so the retained characteristic peaks (02, 11) bands in all the PCH samples in Fig. 1 indicate that lamellar structure is not destructed after the various preparation steps. The first asymmetric reflection in the case of P-C8N12 corresponding to a large d-value (∼4.35 nm) is the result of "house of cards" structure, which indicates the existence of correlated porous structures. The basal reflection at 1.08 nm suggests a collapsed layered structure after calcination, which is indicative of a fail pillaring reaction with OTA^+. The collapsed structure also illustrates that porous structure is formed by the three-dimensional aggregation of clay particles and condensational products of TEOS outside the interlayer space of Mt rather than by the pillaring reaction within the interlamellar space. As for P-C10N12, the basal reflection around 1.29 nm appears as a broad peak indicating that the pillaring reaction is partially and limited performed in interlayer. When alkyl chains contain more than ten carbon atoms, sharp reflections appeared at above 3 nm and broad shoulders around 1.5 nm. Both of the two d-values are resulted from the formation of silica framework within the interlayer of Mt. The two different d-values in one pattern probably due to the inhomogeneity of layer charge. The larger d-value corresponds to the majority with relatively higher layer charge density, and the rest to the lower counterpart. In general, the surfactant with longer alkyl chain tends to have larger basal spacing when it is used to intercalate clay mineral in the same concentration [29] and thus further for PCH. Consequently,

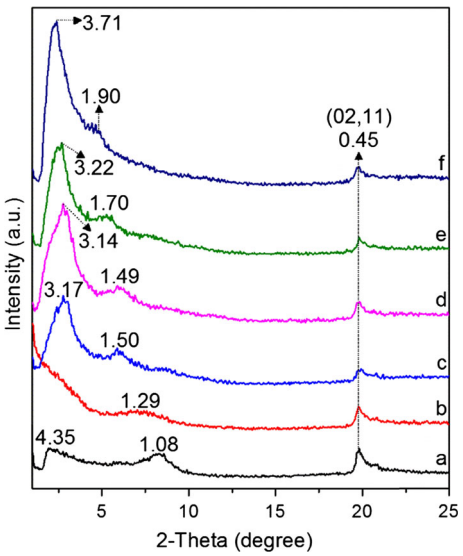

Fig. 1 XRD patterns for PCH samples: *a* P-C8N12, *b* P-C10N12, *c* P-C12N12, *d* P-C14N12, *e* P-C16N12, and *f* P-C18N12

d_{001}-values of PCH samples increase with the ever-increasing organic chain lengths.

3.1.2 Elemental analysis

The carbon contents (f_C) reflects the hydrophobicity degree of interlayer space of OMt. The silica contents (f_{SiO2}) is associated with the Si-framework originated from the polymerization of TEOS within the interlayer of clay. As listed in Table 1, the f_C of OMt gradually increase with the increase of the chain lengths of intercalated surfactants. Increasing the amount of surfactant for the organic intercalation of Mt also improve the f_C of OMt. The trends of change upon f_C illustrate that either increasing the chain length or the amount of intercalation agent leads to the increase of the f_C of OMt. The increased f_C indicate enhanced hydrophobicity of interlayer space and the low f_C of OMt implies weak organophilicity. The hydrophobic degree of interlayer space affects the intercalation of organophilic TEOS. The poor intercalation of TEOS adversely influence the formation of Si-framework within interlayer and further the structural properties of PCH samples. After removing organic templates by calcination, the f_{SiO2} increase from 58.16 % of Mt to the maximum 82.06 % of P-4.0C16N12. The same tendency of f_{SiO2} is observed compared with the corresponding f_C: the larger f_C of OMt correspond to the larger f_{SiO2} of PCH samples. This correlation of f_C and f_{SiO2} indicates the hydrophobic degree of interlayer space has a dramatic effect on the formation of Si-framework. Moreover, increasing chain length of neutral amine leads to a slight increase of f_{SiO2} from 79.7 to 80.4 %, which illustrates the weak modifying effect to interlayer of Mt. In the case of P-C16, the absence of neutral amine results in its lower f_{SiO2} by 8.55 % than that of P-C16N12. The decrease of f_{SiO2} is likely to be attributed to the catalytic effect to polymerization of TEOS [30].

Table 1 Total carbon contents of Mt and OMt and silicon contents of Mt and Mt-derived PCH

Samples	f_C [by mass(%)]	Samples	f_{SiO2} [by mass(%)]
Mt	0	Mt	58.16
Mt-C8	8.31	P-C8N12	70.91
Mt-C10	12.92	P-C10N12	75.55
Mt-C12	15.91	P-C12N12	78.89
Mt-C14	15.73	P-C14N12	79.20
Mt-C16	19.96	P-C16N12	80.06
Mt-C18	21.89	P-C18N12	80.15
Mt-0.5C16	11.54	P-0.5C16N12	74.38
Mt-2.0C16	30.32	P-2.0C16N12	80.99
Mt-4.0C16	32.41	P-4.0C16N12	82.06
		P-C16N8	79.72
		P-C16N14	80.43
		P-C16	71.51

3.1.3 Textural analysis

N_2 adsorption/desorption isotherms for the starting Mt and for PCH obtained with surfactants with different chain lengths and intercalated amount are shown in Fig. 2. The curve for Mt belongs to type IIb according to the IUPAC classification [31] refined by Rouquerol et al. [32], with H3 hysteresis loop characteristic of plate materials possessing non-rigid slit-like pores. After preparation, the isotherms type of PCH samples turns into type IV suggesting the enhanced porosity of PCH samples accompany the pillaring procedures. The hysteresis initially change to H4 and finally back to H3 with the increase of surfactant chain length shown in Fig. 2a. Although the isotherms of PCH samples obviously differ from that of Mt, the type of hysteresis shows slit-shaped pores (H3) and narrow slit-like pores (H4). That is, even after intercalation of cationic surfactant and calcination at 550 °C, the layered structural characteristics of base clay still exist. The gradually increasing adsorbance of N_2 at the same p/p_0 in low partial pressure region of PCH samples from P-C8N12 to P-C18N12 indicates that their microporosities are continuously strengthened by the increased alkyl chain lengths. The type change of hysteresis is mainly related to the degree of pillaring reaction within the interlayer of mineral host. More specifically, the poor porous characteristics of P-C8N12 and P-C10N12 are reflected in their relatively lower adsorbing capacity of N_2 at low partial pressure. The porosities of the two PCH samples do not develop much relative to the parent clay. As for the intermediate samples, the hysteresis loops of P-C12N12 and P-C14N12 show the dual characteristics of type H3 and H4: a long flat plateau of H4 and steep of H3 at high relative pressure. The transitional characters imply the partial and limited pillaring of base clay. Lastly, the types of hysteresis loops of the rest two resultants, P-C16N12 and P-C18N12, return to type H3, which do not exhibit any limiting adsorption at high p/p_0. The unrestricted multilayer adsorption on external surface of P-C16N12 and P-C18N12 most probably corresponds to the enhanced meso- and macroporosity with increasing the chain length of alkyl tails. For the successful Si-pillared clay materials (from P-C12N12 to P-C18N12), the mixed characteristics, of type I and IV, are the most probable consequence of the pore sizes being in the transition range from micro to mesopores [16, 33–35]. Furthermore, in the case of increasing the chain length of neutral amine (Fig. 2b), the isotherms of P-C16N8, P-C16N12, and P-C16N14 do not show much difference except at low p/p_0: the increasing chain length results in the

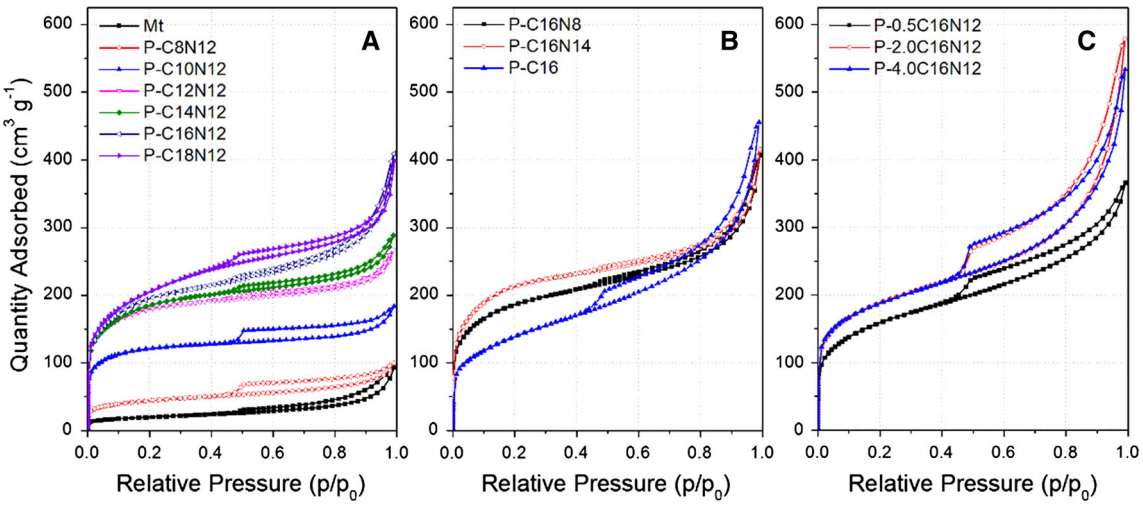

Fig. 2 Nitrogen adsorption/desorption isotherms at −196 °C for Mt and Mt-derived PCH samples

increase of adsorption quantity. The resemblance between the effects of increasing the chain lengths of QAC^+ and amines on the shapes of isotherms of PCH samples (Fig. 2a, b) proves the template effect of neutral amines as co-template agent. In Fig. 2c, the variation (no matter more or less) of the amount of cationic surfactant dramatically increases the meso- and macroporous characteristics of PCH samples, manifesting as the most obvious hysteresis loops [36] and highest values of y-axis among those of all the PCH samples in this work.

The main textural parameters are listed in Table 2, including specific surface area (S_{BET}), microporous specific surface area (S_{micro}), total porous volume (V_{total}), micropore volume (V_{micro}), and average pore diameter (APD). The first three parameters gradually increase as the increase of chain length of surfactant. As for P-C8N12, the exceptionally larger APD is the result of "house of cards" structure [37]. The V_{tatol} of P-C8N12 is not much bigger than that of Mt, while its V_{micro} increased significantly. According to the XRD patterns of Mt and its corresponding products, the layered structure of P-C8N12 becomes collapsed. Therefore, the increased V_{micro} probably stems from the condensation of TEOS outside the interlayer rather than that within the interlayer of clay. Similarly, the V_{micro} of P-C10N12 further increases in comparison with that of P-C8N12 due to its partially pillared structure. For surfactants with more than ten carbon atoms in their hydrophobic tails, progressive increases of all the textural parameters are regularly driven by the ever-increasing alkyl chain lengths. The analogous tendency is also observed when the chain length of neutral amine increased: the longer alkyl chain is, the larger the textural parameters are. Furthermore, all the textural parameters of PCH made from Mt-0.5C16 are smaller than that of P-C16N12,

Table 2 Textural characteristics of initial and treated montmorillonite samples

Sample	S_{BET} ($m^2\ g^{-1}$)	S^a_{micro} ($m^2\ g^{-1}$)	V^b_{total} ($cm^3\ g^{-1}$)	V^a_{micro} ($cm^3\ g^{-1}$)	APD (nm)
Mt	69.5	62.3	0.119	0.028	6.9
P-C8N12	155.5	156.5	0.138	0.075	3.6
P-C10N12	452.3	442.1	0.265	0.204	2.3
P-C12N12	655.8	646.4	0.386	0.302	2.4
P-C14N12	661.0	658.4	0.420	0.317	2.5
P-C16N12	690.1	681.6	0.550	0.334	3.2
P-C18N12	720.1	751.4	0.539	0.379	3.0
P-C16N8	665.1	642.5	0.549	0.308	3.3
P-C16N14	784.6	734.6	0.557	0.361	2.8
P-0.5C16N12	549.1	557.9	0.524	0.293	3.8
P-2.0C16N12	668.3	707.4	0.804	0.359	4.8
P-4.0C16N12	670.8	708.9	0.732	0.355	4.4
P-C16	467.8	547.2	0.618	0.302	5.3

[a] From Dubinin–Astakhov (DA) equation

[b] From the amount adsorbed at the relative pressure of 0.97

attributed to the less hydrophobic modification of Mt-0.5C16. When the amount of cationic surfactant is more than one time CEC of Mt, the enhanced hydrophobicity attracts more introduction of TEOS into the interlayer space. The decreased S_{BET} suggests that the excessive TEOS might partially block the porous structure. However, the amount of template agent increased after all, by which the pore volume of the products mainly increase from mesopores volume.

Porous clay heterostructures in this work has a combined micro- and mesoporosity, and thus the NLDFT method has to be adopted to characterize the PSD for PCH samples. As shown in Fig. 3, peaks near 1.3 nm shown in

all the PCH samples correspond to pores generated by the pillaring reaction. The invariability of most probable pore size (MPPS) illustrates that changing the length of aliphatic chain does not affect the major pore size of PCH samples, though longer chain of QAC^+ brings about the more distinct distribution near 1.3 nm and concentrated PSD in mesopore region. The same variation tendency is also found in changing the chain length of neutral amine (Figs. 3e, 4a, b). The unchanged MPPS in present work is different from conventional outcomes evaluated by Horvath–Kawazoe analysis [4], and BJH method [19, 20]. When increasing (or decreasing) the amount of CTAB, MPPS slightly moves to about 1.4 nm (Fig. 4c–e), which means micropore diameter increased to around 1.4 nm. P-C16 is the product prepared without DDA, the PSD of which appear discrete compared with the one obtained with DDA, P-C16N12 (Figs. 3e, 4f). This comparison is abnormal for the template effect of neutral amine. Introducing DDA as co-template agent results in more occupation of interlayer space, which should have meant the same discrete PSD in mesopore region to that of P-2.0C16N12 and P-4.0C16N12. However, more concentrated PSD in P-C16N12 are contradictory to the preceding variation tendency, which reveals that neutral amine not only served as template but also as other functional agents.

3.2 Formation of porous structure and pore size control by template agent

As for structural and textural characteristics, the two-dimensional framework of porous silica intercalated between clay layers is considered to derive from the interactions between the surfactants and silicate ions introduced into the interlayer space. The interactions cause the rod-like micellar assemblies of QAC^+ and neutral amine surrounded by hydrated silica structures [4]. This conventional explanation for the formation of porous structure of PCH can be called micellar template model. The organic modification of inorganic clay minerals, as an important step to prepare PCH, has a great influence on

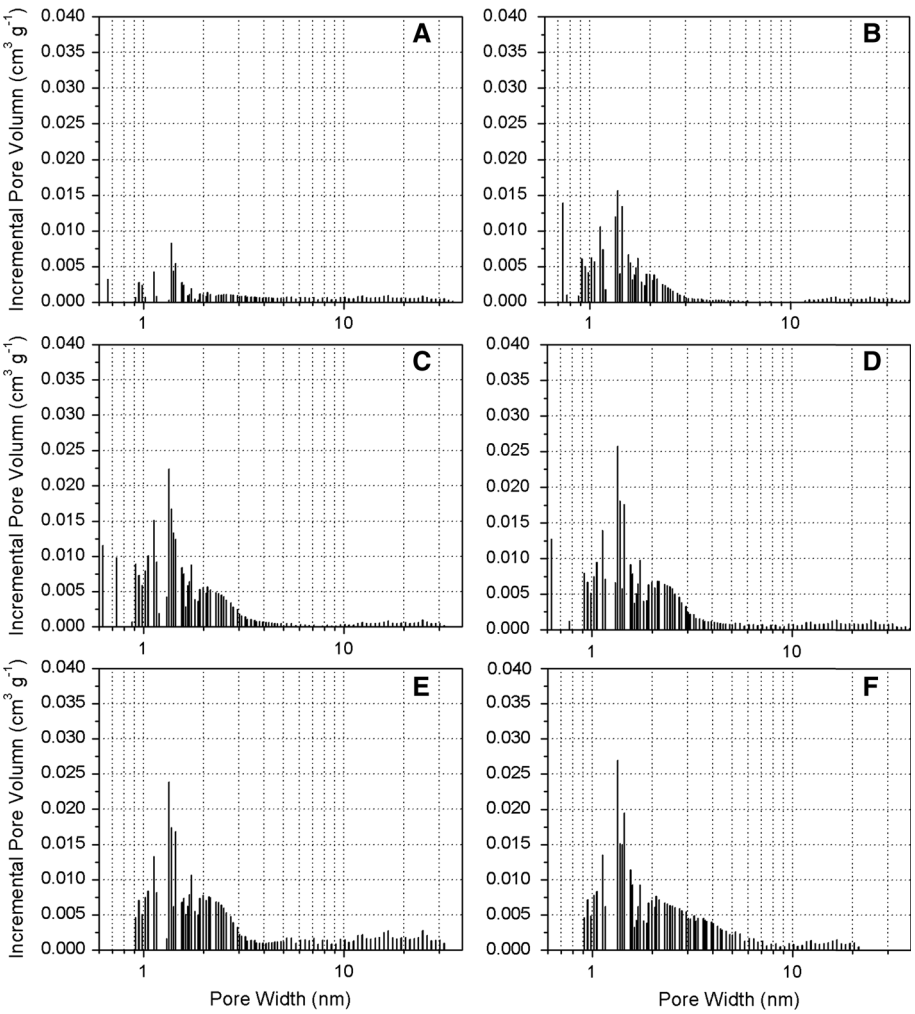

Fig. 3 Pore size distribution patterns for PCH samples: **a** P-C8N12, **b** P-C10N12, **c** P-C12N12, **d** P-C14N12, **e** P-C16N12, and **f** P-C18N12

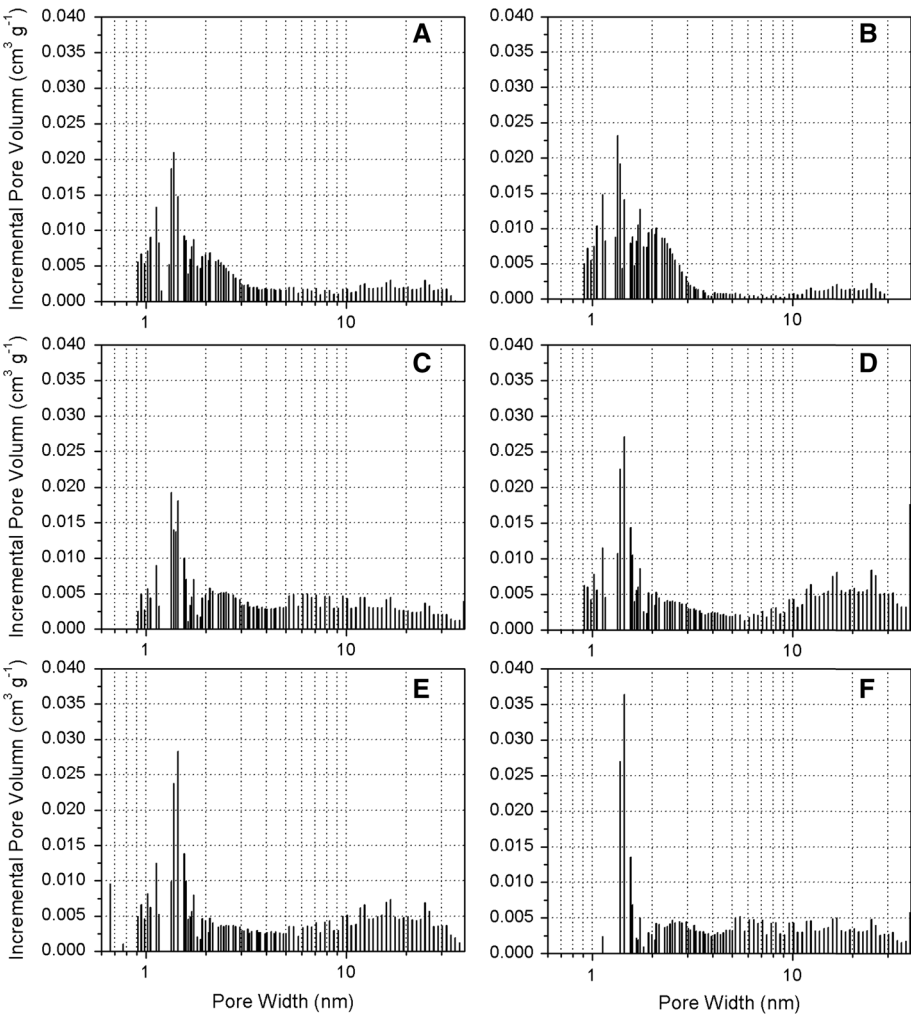

Fig. 4 Pore size distribution patterns for PCH samples: **a** P-C16N8, **b** P-C16N14, **c** P-0.5C16N12, **d** P-2.0C16N12, **e** P-4.0C16N12, and **f** P-C16

PSD. In previous study [4, 16], changing the chain length of either QAC^+ or neutral amine leads to the change of pore size: the longer chain results in the larger pore in diameter. This phenomenon is based on the key assumption of formation and assembly of rod-like micellar within interlayer. Micelle is formed by the spontaneous and ordered aggregation of dissolved amphiphilic surfactants in solvents. Polar solvents correspond to micelle, and the apolar to reversed micelle. During the preparation of PCH-processor (PCH before calcination), OMt was initially dispersed in a mass of TEOS, hence the environment for QAC^+ within interlayer is apolar. Even if micelle can form in interlayer, micellar type should be the reversed one. The formation of micelle depends on the three primary forces, namely, hydrophobic repulsion between the hydrocarbon chains and the aqueous environment, charge repulsion of ionic head groups, and the van der Waals attraction between the alkyl chains [38]. Similarly, reversed micelle is the result of the latter two forces and the organophobic repulsion between the hydrophilic ammonium head groups of QAC^+ and the apolar environment. In the confined interlayer space, the fourth force also influences the formation of reversed micelle: charge attraction between positively charged head groups and negatively charged clay layer. The intensively electrostatic force restricts the mobility of ammonium head groups and makes them tend to be preferentially positioned on siloxane surface [39, 40]. Furthermore, the reversed micelle is formed in water-in-oil emulsion. The increase of total carbon contents within interlayer continually enhances the hydrophobicity of OMt, which leads to less interlayer water supporting the formation of "water pool" in the center of reversed micelle. Moreover, as for the reversed micelle with low water concentrations, the water molecules fill the hydration sphere of the counter ion so that solubilized analytes encounter a more viscous, less polar environment than in ordinary bulk water [38]. However, little counter ion (Br^- and Cl^-) exists within interlayer when the amount of cationic surfactant is no more than one time CEC of Mt. In the case of Mt-2.0C16 and Mt-4.0C16, the hydrophobic tails

within interlayer arrange more densely than Mt-C16, thus enhancing van der Waals attraction between the tails. This enhanced attraction adversely affects the formation of reversed micelle. Consequently, the microenvironment of OMt within interlayer does not support the formation of reversed micelle.

Excluding the possibility of reversed micelle forming within interlayer, another type of surfactant aggregation should exist and result in the formation of porous structure. When OMt is wetted by a big dose of organic solvent, the solvent molecules permeate into the interlayer of OMt accompanied by the easy swell and disperse of OMt in organic medium (Fig. 5b). Only the alkyl chains containing no less than 10 carbon atoms can make the corresponding OMt swell well. If short-chain organic cations are used, the organic derivatives will not swell and lack organophilicity [41, 42]. This conclusion explains the poor textural properties of PCH prepared with OTA^+ and DTA^+. In the case of long chains with more than ten carbon atom, TEOS monomers enter into the spacer between the interlayer organic long-chains and partially displace them. As a result, the hydrocarbon tails congregate together due to the extrusion and occupation of interlayer space by the polymerizate of TEOS, while the cationic head group positions on the siloxane surface without much mobility (Fig. 5c). The aggregates from organic template agents with different length of chains seems to be mainly composed of relatively fixed number of alkyl chains according to the same MPPS.

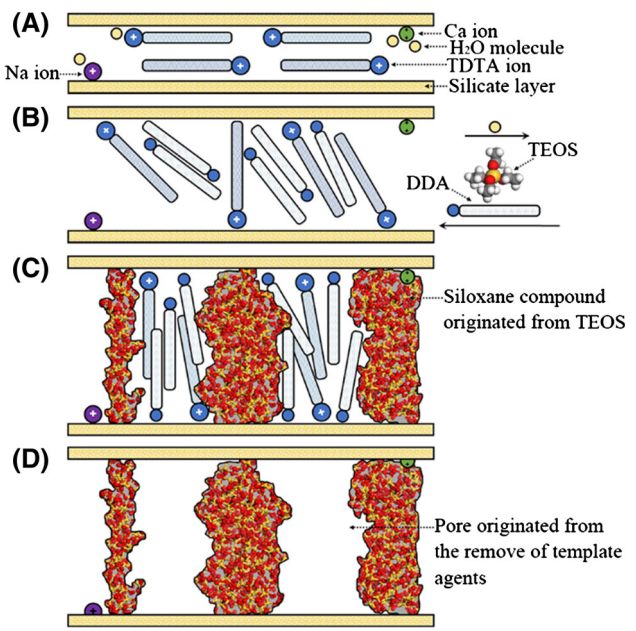

Fig. 5 Proposed mechanism for the formation of porous structure of PCH: **a** intercalation of $TDTA^+$, **b** intercalation of DDA and TEOS, **c** formation of inorganic pillars within interlayer, and **d** calcinated PCH with a 2D Si-framework between the clay layers

Due to the catalytic effect of neutral amine [30], the polymerization of TEOS monomers to oligomers and to polymers within interlayer is more rapid than that outside the interlayer. Therefore, the polymerization of TEOS within interlayer is more complete. Finally, pillars within interlayer from the polymerization of TEOS constitute the two-dimensional framework of porous silica after calcination (Fig. 5d). This explanation for the formation of porous structure of PCH can be referred as non-micellar template model.

The pore size of PCH is not associated with the carbon loadings within interlayer of OMt as discussed above. The total carbon contents and surfactant distribution within interlayer depend on the nature of base clay (layer charge density) and intercalation agent (chain length and number of long chain) as well as the mixture ratio of organic surfactant and inorganic clay mineral host. Assuming evenly distribution of the layer charges and the homogeneous intercalation of surfactant, the longer alkyl chain and larger intercalated amount of surfactant imply the more fully filling of interlayer space and larger pore volume. However, the larger carbon loadings do not result in the gradual increase of the MPPS (Figs. 3, 4a, b). A more reasonable explanation is proposed that the increased carbon loadings cause the increase of pore volume of PCH in depth dimension rather than in diameter dimension. Although the PSD of PCH samples in micropore region do not change much with the increasing carbon contents within interlayer, it is undeniable that the trend of change on the major textural parameters is precisely the same to the previous results mentioned above. Therefore, the results of structural and textural properties of PCH samples in this paper are not contradictory to the results in previous works. According to the present result, the pore size control by template agent are mainly reflected by the variation of pore volume rather than MPPS in micropore region.

3.3 Roles of inorganic base clay and long-chain organic template agents in the formation of porous structure

Porous clay heterostructures belong to pillared interlayered clays (PILC). The base clay supplies the pillaring objective and space like other PILC samples, e.g. Al-PILC and organo montmorillonite. Both exterior clay layers and incorporated pillars constitute the porous structure. Differing from the M41S family mesoporous materials, the nature of the clay mineral host affects the arrangement and orientation of alkyltrimethylammonium salt within interlayer and restricts the mobility of cationic head groups. Therefore, the surfactants could not congregate to form micelle within interlayer even if in aqueous solution [43], but to form interlayer surfactant aggregates. The interlayer

environment also does not support the formation of reversed micelle in apolar medium. Consequently, the aggregation type of organic template agent is significantly affected by parent material. In addition, researchers pin their hopes on layer charge density of clay to bring about substantial changes in the lateral interpillar distances [44–46]. Layer charge density directly affects organic carbon loadings and arrangement of hydrocarbon chain within interlayer [47]. If the layer charge reduction occurs in a homogeneous manner, the variation in layer charge density will influence the packing density of alkyl chains, and probably further affect PSD of PCH samples. Further research and supporting data is needed for the deduction.

Both cationic surfactant and neutral amine as template agents for synthesis of PCH help with the formation of porous structure. According to the presented results, QAC^+ plays a significant role in forming pores by replacing the inorganic interlayer cations. The replacement changes the hydrophilic silicate surface into hydrophobic and enlarges basal spacing so that the interlayer is accessible for TEOS. The loadings of cationic surfactant have a significant effect on textural properties of PCH. Shorter chain and lower intercalated amount of QAC^+ cause the poor pillaring interaction, while longer chain ($\geq$10 carbon atoms) and larger intercalated amount result in better textural properties. On the other hand, neutral amine is not the dominant factor for the formation of pores. The porous structure still formed even for synthesizing PCH without neutral amine, though the resultant had wider PSD in mesopore region (Fig. 4f). The addition of neutral amine leads to a more concentrated PSD, especially in mesopore region, due to the catalytic effect of polymerizing TEOS. Moreover, the increasing trend of textural parameters caused by increasing the chain length of neutral amine is similar to that of QAC^+, which shows the co-template effect of neutral amine.

4 Conclusions

In this work, the effect of organic templates on the structural properties of PCH was investigated. The appearances of non-basal reflections of PCH samples in XRD patterns indicated that the lamellar structure was still retained after the preparation procedure. By the result of elemental analysis, f_{SiO2} of PCH samples increased with the increase of f_C of the corresponding OMt. This positive correlation was due to the enhanced hydrophobicity of OMt beneficial to the introduction of TEOS into interlayer of base clay. The major textural parameters of PCH samples gradually increased with increasing the carbon loadings of OMt, while the MPPS of PCH remained unchanged around 1.3–1.4 nm, which suggested that the increased pore volume of PCH was in depth dimension rather than in diameter dimension.

The non-micellar template model was proposed to explain the formation mechanism of porous structure of PCH according to the structural and chemical component results. In this model, the inorganic base clay changed the congregation type of organic templates within interlayer. The hydrocarbon tails congregated together because of the extrusion and occupation of polymerizate of TEOS in interlayer space. The aggregates from organic template agents with different length of chains seemed to be mainly composed of relatively fixed number of alkyl chains according to the unchanged MPPS. TEOS monomers entered into the spacer between the aggregates to conduct pillaring reaction, resulting in the formation of porous structure. The cationic surfactant played a significant role as the template agent in forming pores, whose arrangement and orientation was controlled by the base clay. The surfactant changed hydrophilic silicate surface of mineral host into hydrophobic and enlarged the basal spacing so that the interlayer was accessible for TEOS. The neutral amine was not the dominant factor for the formation of pores. However, its catalysis for the condensation of TEOS led to a more concentrated PSD especially in mesopore region.

Acknowledgments Supported by the Strategic Priority Research Program of the Chinese Academy of Sciences (Grant No. XDB05050200), National Key Technology Research and Development Program of the Ministry of Science and Technology of China (Grant No. 2013BAC01B02), Team Project of Natural Science Foundation of Guangdong Province, China (Grant No. S2013030014241), and the National Natural Science Foundation of China (Grant Nos. 41272060, 41102022). The authors also thank W. W. Yuan and W. B. Yu for the valuable discussions. This is a contribution (No. IS-1969) from GIGCAS.

References

1. D.Y. Zhao, J.L. Feng, Q.S. Huo, N. Melosh, G.H. Fredrickson, B.F. Chmelka, G.D. Stucky, Science **279**(5350), 548 (1998)
2. X.Y. Liu, B.Z. Tian, C.Z. Yu, F. Gao, S.H. Xie, B. Tu, R.C. Che, L.M. Peng, D.Y. Zhao, Angew. Chem. Int. Ed. **41**(20), 3876 (2002)
3. J.S. Beck, J.C. Vartuli, W.J. Roth, M.E. Leonowicz, C.T. Kresge, K.D. Schmitt, C.T.W. Chu, D.H. Olson, E.W. Sheppard, S.B. Mccullen, J.B. Higgins, J.L. Schlenker, J. Am. Chem. Soc. **114**(27), 10834 (1992)
4. A. Galarneau, A. Barodawalla, T.J. Pinnavaia, Nature **374**(6522), 529 (1995)
5. R.A. Schoonheydt, T. Pinnavaia, G. Lagaly, N. Gangas, Pure Appl. Chem. **71**(12), 2367 (1999)
6. M. Zimowska, H. Palkova, J. Madejova, R. Dula, K. Pamin, Z. Olejniczak, B. Gil, E.M. Serwicka, Microporous Mesoporous Mater. **175**, 67 (2013)
7. L. Chmielarz, Z. Piwowarska, P. Kustrowski, A. Wegrzyn, B. Gil, A. Kowalczyk, B. Dudek, R. Dziembaj, M. Michalik, Appl. Clay Sci. **53**(2), 164 (2011)

8. M. Munoz, G. Sathicq, G. Romanelli, S. Hernandez, C.I. Cabello, I.L. Botto, M. Capron, J. Porous Mater. **20**(1), 65 (2013)
9. F. Qu, L.Z. Zhu, K. Yang, J. Hazard. Mater. **170**(1), 7 (2009)
10. C.D. Nunes, J. Pires, A.P. Carvalho, M.J. Calhorda, P. Ferreira, Microporous Mesoporous Mater. **111**(1–3), 612 (2008)
11. L.Z. Zhu, S.L. Tian, Y. Shi, Clay Clay Miner. **53**(2), 123 (2005)
12. N. Bunnak, S. Ummartyotin, P. Laoratanakul, A.S. Bhalla, H. Manuspiya, J. Porous Mater. **21**(1), 1 (2014)
13. C. Santos, M. Andrade, A.L. Vieira, A. Martins, J. Pires, C. Freire, A.P. Carvalho, Carbon **48**(14), 4049 (2010)
14. D. Nguyen-Thanh, T.J. Bandosz, Microporous Mesoporous Mater. **92**(1–3), 47 (2006)
15. Z.B. Wu, J.C. Tian, Z.M. Liu, P. Tian, L. Xu, Y. Yang, Y.Y. Zhang, X.H. Bao, X.M. Liu, X.C. Liu, J Porous Mater. **13**(1), 73 (2006)
16. J. Pires, A.C. Araujo, A.P. Carvalho, M.L. Pinto, J.M. Gonzalez-Calbet, J. Ramirez-Castellanos, Microporous Mesoporous Mater. **73**(3), 175 (2004)
17. H.Y. Zhu, X.S. Zhao, G.Q. Lu, D.D. Do, Langmuir **12**(26), 6513 (1996)
18. H.Y. Zhu, P. Cool, E.F. Vansant, Recent Adv Sci. Technol. Zeol. Relat. Mater. Pts A C **154**, 1456 (2004)
19. L.M. Wei, T. Tang, B.T. Huang, Microporous Mesoporous Mater. **67**(2–3), 175 (2004)
20. M. Nakatsuji, R. Ishii, Z.M. Wang, K. Ooi, J. Colloid Interface Sci. **272**(1), 158 (2004)
21. X.R. Hu, G.L. Lu, Y. Yang, Chinese J. Anal. Chem. **28**(11), 1402 (2000)
22. L.Z. Zhu, R.L. Zhu, L.H. Xu, X.X. Ruan, Colloid Surf. A **304**(1–3), 41 (2007)
23. X.H. Li, Z.X. Li, M.T.D. Wingate, S.L. Chung, Y. Liu, G.C. Lin, W.X. Li, Precambrian Res. **146**(1–2), 1 (2006)
24. S.J. Gregg, K.S.W. Sing, *Adsorption, Surface Area, and Porosity*, 2nd edn. (Academic Press, New York, 1982)
25. A. Gil, P. Grange, Colloid Surf. A **113**(1–2), 39 (1996)
26. J.P. Olivier, M.L. Occelli, J. Phys. Chem. B **105**(3), 623 (2001)
27. M.A. Vicente, A. Gil, F. Bergaya, in *Developments in Clay Science*, ed. by B. Faïza, L. Gerhard (Elsevier, Amsterdam, 2013), p. 523
28. G. Lagaly, M. Ogawa, I. Dékány, in *Developments in Clay Science*, ed. by B. Faïza, L. Gerhard (Elsevier, Amsterdam, 2013), p. 435
29. L.B. de Paiva, A.R. Morales, F.R.V. Diaz, Appl. Clay Sci. **42**(1–2), 8 (2008)
30. J.P. Blitz, R.S.S. Murthy, D.E. Leyden, J. Colloid Interface Sci. **126**(2), 387 (1988)
31. K.S.W. Sing, D.H. Everett, R.A.W. Haul, L. Moscou, R.A. Pierotti, J. Rouquerol, T. Siemieniewska, Pure Appl. Chem. **57**(4), 603 (1985)
32. F. Rouquerol, J. Rouquerol, K.S.W. Sing, G. Maurin, P. Llewellyn, in *Adsorption by Powders and Porous Solids*, 2nd edn., ed. by F. Rouquerol, J. Rouquerol, K.S.W. Sing, P. Llewellyn, G. Maurin (Academic Press, Oxford, 2014), p. 1
33. M. Polverejan, Y. Liu, T.J. Pinnavaia, Chem. Mater. **14**(5), 2283 (2002)
34. R. Ishii, M. Nakatsuji, K. Ooi, Microporous Mesoporous Mater. **79**(1–3), 111 (2005)
35. J. Pires, M. Pinto, J. Estella, J.C. Echeverria, J. Colloid Interface Sci. **317**(1), 206 (2008)
36. P. Yuan, D. Liu, M.D. Fan, D. Yang, R.L. Zhu, F. Ge, J.X. Zhu, H.P. He, J. Hazard. Mater. **173**(1–3), 614 (2010)
37. T.J. Pinnavaia, M.S. Tzou, S.D. Landau, R.H. Raythatha, J. Mol. Catal. **27**(1–2), 195 (1984)
38. L.J.C. Love, J.G. Habarta, J.G. Dorsey, Anal. Chem. **56**(11), 1132 (1984)
39. H. Heinz, R.A. Vaia, R. Krishnamoorti, B.L. Farmer, Chem. Mater. **19**(1), 59 (2007)
40. Q. Zhao, S.E. Burns, Langmuir **28**(47), 16393 (2012)
41. V.N. Moraru, Appl. Clay Sci. **19**(1–6), 11 (2001)
42. J.W. Jordan, J. Phys. Colloid Chem. **53**(2), 294 (1949)
43. J.X. Zhu, L.Z. Zhu, R.L. Zhu, B.L. Chen, Clay Clay Miner. **56**(2), 144 (2008)
44. H. Nijs, M. De Bock, N. Maes, E.F. Vansant, J Porous Mater. **6**(4), 307 (1999)
45. M.M. Herling, H. Kalo, S. Seibt, R. Schobert, J. Breu, Langmuir **28**(41), 14713 (2012)
46. A. Baumgartner, F.E. Wagner, M. Herling, J. Breu, Microporous Mesoporous Mater. **123**(1–3), 253 (2009)
47. H.P. He, Y.H. Ma, J.X. Zhu, P. Yuan, Y.H. Qing, Appl. Clay Sci. **48**(1–2), 67 (2010)